

Analysis of Radionuclide Releases from the Fukushima Dai-ichi Nuclear Power Plant Accident Part II

PASCAL ACHIM,¹ MARGUERITE MONFORT,¹ GILBERT LE PETIT,¹ PHILIPPE GROSS,¹ GUILHEM DOUYSSSET,¹
THOMAS TAFFARY,¹ XAVIER BLANCHARD,¹ and CHRISTOPHE MOULIN¹

Abstract—The present part of the publication (Part II) deals with long range dispersion of radionuclides emitted into the atmosphere during the Fukushima Dai-ichi accident that occurred after the March 11, 2011 tsunami. The first part (Part I) is dedicated to the accident features relying on radionuclide detections performed by monitoring stations of the Comprehensive Nuclear Test Ban Treaty Organization network. In this study, the emissions of the three fission products Cs-137, I-131 and Xe-133 are investigated. Regarding Xe-133, the total release is estimated to be of the order of 6×10^{18} Bq emitted during the explosions of units 1, 2 and 3. The total source term estimated gives a fraction of core inventory of about 8×10^{18} Bq at the time of reactors shutdown. This result suggests that at least 80 % of the core inventory has been released into the atmosphere and indicates a broad meltdown of reactor cores. Total atmospheric releases of Cs-137 and I-131 aerosols are estimated to be 10^{16} and 10^{17} Bq, respectively. By neglecting gas/particulate conversion phenomena, the total release of I-131 (gas + aerosol) could be estimated to be 4×10^{17} Bq. Atmospheric transport simulations suggest that the main air emissions have occurred during the events of March 14, 2011 (UTC) and that no major release occurred after March 23. The radioactivity emitted into the atmosphere could represent 10 % of the Chernobyl accident releases for I-131 and Cs-137.

Key words: Fukushima Dai-ichi accident, atmospheric transport modeling, source terms evaluation, Cs-137, I-131, Xe-133, CTBTO.

1. Introduction

On March 11, 2011, the tsunami induced by the 9.0 magnitude earthquake that occurred east of Japan caused serious damage to the cooling systems of the Fukushima Dai-ichi Nuclear Power Plant (NPP). Due to the lack of cooling, hydrogen and vapor blasts, dewatering of spent fuel rod pools and fires led to the release of radioactive materials into the atmosphere.

Although at the time this article was written, the comprehensive understanding of the accident was not fully established, it was accepted that units 1, 2 and 3 reached a fuel fusion state. The detection in the air of fission and activation products by monitoring stations belonging to the International Monitoring System (IMS) of the Comprehensive Nuclear Test Ban Treaty Organization (CTBTO) is likely to provide relevant information on the reactor core damage. CEA relied on these IMS data and on analysis performed by radionuclide laboratories supporting the CTBT network in order to estimate the worldwide distribution of the atmospheric releases of radioactive material and to better understand the accident features. The first part (Part I) of this study is dedicated to observations and interpretations of the accident characteristics relying on the chronology of the major detections and the nature of detected radionuclides (LE PETIT *et al.*, 2012). This linked part (Part II) deals with the Atmospheric Transport Modeling (ATM) at global scale (long range simulations). The objective is to assess the arrival time of radionuclides over IMS stations and to evaluate the quantities released into the atmosphere. We will mainly focus on Cs-137, I-131 and Xe-133 fission products. Hence, the two first radionuclides will be the main contributors to dose and worldwide industrial Xe-133 background could be modified by Fukushima radionuclide release affecting the performances of the CTBT radionuclide monitoring network.

2. Sequence of the Accident and Observations at Fukushima Dai-ichi Site

After the automatic shutdown of the reactors, cooling problems were caused by the March 11

¹ CEA, DAM, DIF, 91297 Arpajon, France. E-mail: pascal.achim@cea.fr

tsunami. During venting operations on several units, hydrogen explosions and fires occurred. Table 1 gives the sequence of main events that could have led to the release of radionuclides into the atmosphere (Japanese Nuclear and Industrial Safety Agency, NISA; OKADA, 2011; Ministry of Education, Culture, Sports, Science and Technology, MEXT). Four of the six units were damaged as a result of the tsunami. Only units 1, 2 and 3 were in operation at the time of the event. As unit 4 had been already stopped, it was not involved in venting operations and did not suffer an hydrogen explosion. However, it was damaged by the explosion of unit 2 leading to a fire in the spent fuel storage pool. It should be noted that other events than those mentioned in Table 1 could have led to atmospheric emissions, like cooling operations by spraying water from helicopters or terrestrial devices that could have resuspended small quantities of radionuclides.

2.1. Dose Rate Measurements

Figure 1 shows the evolution of the dose rates measured during March 2011 on the monitoring points located on the Fukushima Dai-ichi site (TEPCO Press releases). The monitoring points are approximately located 1 km away from the reactors. Measurement of amplitude over time depends on both

the amount of material released in the atmosphere and the location of the monitoring stations with regard to the prevailing wind. Since the time series are incomplete, they may not represent all the events that could have occurred. However, measurements show a succession of peaks of dose rate, which can be related to the events presented in Table 1. Releases that led to the highest measured dose rates took place on March 14 and 15 UTC (events 7–11 in the table). After March 25, dose rates decrease continuously with time. Even though they give an indication of release timing, dose rates are difficult to interpret since they do not allow the identification of radionuclides. Hence, dose rates partly result from the contribution of short half-life radionuclides such as I-132 (2.295 h) (QUÉLO *et al.*, 2011). In addition, dose rate monitoring devices are subject to saturation phenomena, thus making the interpretation of the relative peak amplitudes difficult.

2.2. Assessment of Atmospheric Cs-137 and I-131 Leakage after March 22

From March 22, measurements of activity concentrations in Cs-137 and I-131 were conducted at the Fukushima Dai-ichi site by the TEPCO Company (TEPCO Press releases) (Fig. 2, left). These measurements were made daily from mobile sampling

Table 1

Sequence of main identified events that could have lead to atmospheric releases

Date (UTC)	Concerned unit	Events
03/11 05:46		Automatic shutdown of units 1, 2 and 3 due to earthquake
03/12 01:17	Unit 1	1) Venting
03/12 06:36	Unit 1	2) Hydrogen explosion in reactor building
03/12 23:41	Unit 3	3) Venting
03/13 02:00	Unit 2	4) Venting
03/13 20:20	Unit 3	5) Venting
03/14 02:01	Unit 3	6) Hydrogen explosion in reactor building
03/14 15:02	Unit 2	7) Venting
03/14 21:15	Unit 2	8) Explosion. Possible damage of pressure system. Damage of building wall of unit 4 reactor
03/15 00:38	Unit 4	9) Fire occurred in spent fuel cooling pool
03/15 20:45	Unit 4	10) Fire occurred in spent fuel cooling pool
03/15 23:20	Unit 3	11) White smoke generated
03/20 02:00	Unit 3	12) Rise of primary containment vessel pressure
03/21 06:55	Unit 3	13) Greyish smoke
03/23 07:20	Unit 3	14) Black smoke

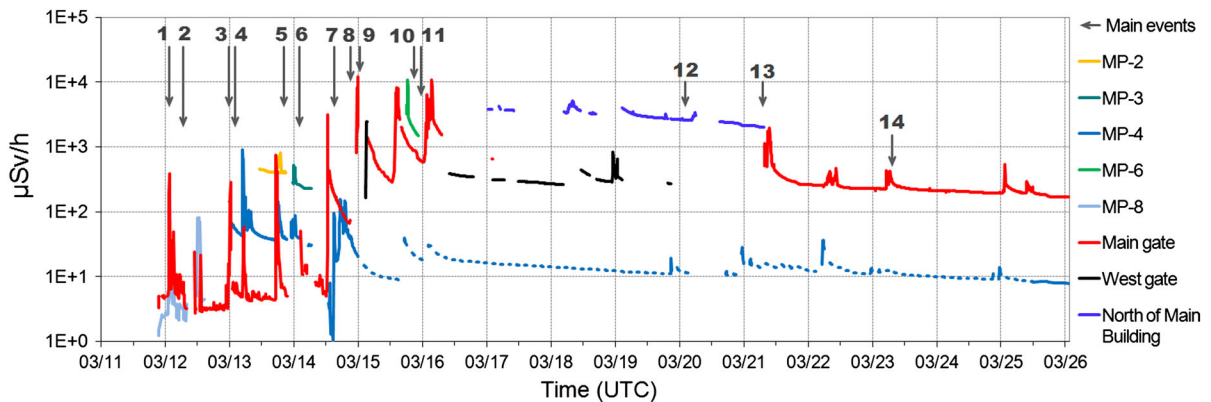


Figure 1

Dose rates measured on the monitoring points located around the Fukushima plant. Events identified in Table 1 are shown by the arrows

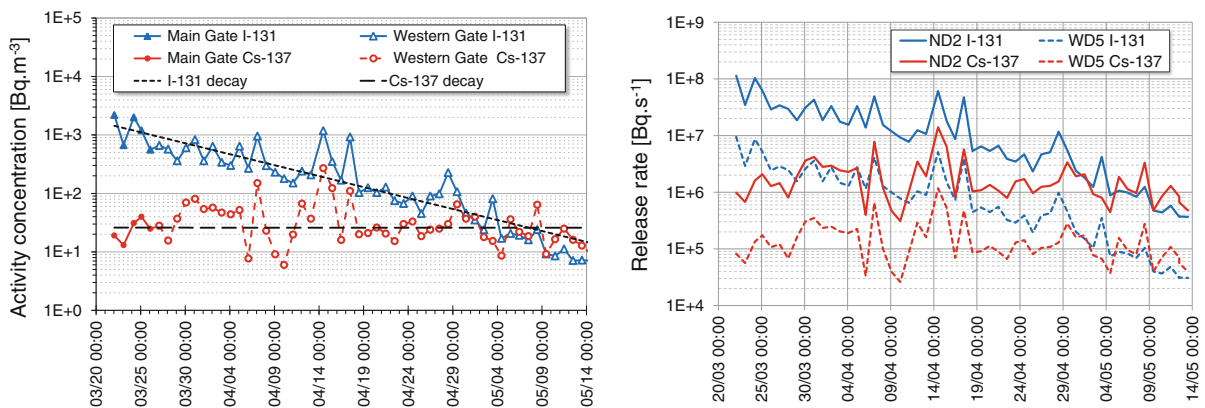


Figure 2

Left activity concentrations measured on the Fukushima Dai-ichi site for I-131 and Cs-137. Right estimated release rates (Gaussian formulation) required to match measurements. ND normal diffusion; WD weak diffusion; 2 and 5 refer to wind speed (m/s)

devices located near the so-called monitoring points “Western Gate” and “Main Gate”. Gamma spectroscopy measurements were performed at the Fukushima Dai-ichi site. Measurements show that the I-131 activity concentrations decrease with time following approximately the radioactive decay of the radionuclide, with some exceptions, such as the period from April 13 to 19. Concerning Cs-137, measured activity concentrations appear fairly constant, in agreement with the half-life of the radionuclide. This result points out that no major release has been measured by these monitoring devices after March 22 and rather indicates a continuous release of radionuclides into the atmosphere at a constant emission factor.

Figure 2 (right) provides rough estimation of release rates required to obtain measurements presented in Fig. 2 (left). Release rates are calculated from a Gaussian dispersion formulation, assumed to be relevant due to the small distance between the reactors and the monitoring devices. It is assumed that sensors were under the direct influence of releases, which was not necessarily the case in reality. Building effects on dispersion are not taken into account and ground deposition and radioactive decay phenomena are neglected (both are negligible at short distances for considered radionuclides). Calculations are performed for a 20 m high source and for two meteorological conditions assumed to provide reasonable major and minor estimations of

release rates: i.e., unstable atmosphere with a 2 m s^{-1} wind speed (Normal Diffusion 2) and a stable atmosphere with a 5 m s^{-1} wind speed (Weak Diffusion 5). By time integration of the release rates over the observation period (~ 2 months from March 22), these two conditions lead to releases ranging from 1×10^{13} to 1×10^{14} Bq for I-131 and from 1×10^{12} to 1×10^{13} Bq for Cs-137. The work should be continued to estimate the amounts released during leaks (i.e., between main releases) that may have occurred before March 22.

3. Elements on Atmospheric Transport Modeling (ATM)

ATM has been conducted at both the regional (short range simulations) and global scale (long range simulations). This section describes briefly the methodologies used and the objectives of the simulations.

3.1. Short Range Simulations

The regional scale simulations have been conducted using MM5 V3.7 (MM5, 2005) and WRF V3.3 (WRF website) mesoscale meteorological models. These well-known systems are parallelized, limited area, non hydrostatic, terrain following and sigma-coordinate models designed to simulate or predict mesoscale atmospheric circulation. NCEP's Global Forecast System (GFS) meteorological data with 6 h and 0.5° resolutions have been used as initialization and boundary conditions (National Centers for Environmental Prediction/GFS website). Among the existing atmospheric dispersion models, the 3D lagrangian particle dispersion model (LPDM) FLEXPART was used (STOHL *et al.*, 1998; FLEXPART homepage). The versions of the model used here are those specifically developed for MM5 (V.6.2) and WRF (FAST and EASTER, 2006). It should be noted that in the standard WRF FLEXPART version, wet deposition phenomena are not fully implemented. To correct this, the calculation of precipitation subgrid variability was made available in particular the calculation of the fraction of surface that undergoes precipitation. This fraction is a function of convective

and large-scale precipitation and also depends on cloud cover. The method developed is based on the MM5 FLEXPART model, where cloud cover is estimated from the total water contained in the air column between ground and roof level of the calculation domain.

Regional calculations were carried out to simulate, at the scale of a few hundreds kilometers, the dispersion of radionuclides emitted by Fukushima Dai-ichi NPP. In particular, one goal was to simulate dry and wet deposits and to compare results with measured dose rates in the Ukedo river basin located on the northwest region of the Fukushima Dai-ichi site (DOE, 2011). Because of their spatial and temporal resolutions, long range models are not able to reproduce this event (TAKEMURA *et al.*, 2011). Unfortunately, the mesoscale simulations driven by 0.5° GFS failed to reproduce the observed deposits. They were caused by a low rainfall washout of the radionuclide plume emitted at the end of March 14 (UTC) following the venting and hydrogen explosion that occurred on unit 2 (OKADA, 2011). While the prevailing wind directions were mainly from the northwest and northeast, the release occurred in a southeast flow during a short duration, which was not reproduced in the simulations because of shortcomings in GFS data. However, no other better large-scale data were found for the characterization of these meteorological conditions (MATHIEU *et al.*, 2012). Figure 3 shows an example of a comparison between observations and simulations at the Fukushima Airport (RJSF station, 37.2275N ; 140.4281E), located 60 km southwest of Fukushima Dai-ichi NPP. In this example, the WRF mesoscale wind field has a resolution of 1.6 km and 1 h. This figure shows that the southeast wind observed during the early hours of March 15 is not reproduced by the model (similar result has been obtained with MM5).

Several mesoscale simulation attempts were performed by varying the vertical calculation grid resolution and the relaxation coefficients towards the large-scale input data inside and outside the boundary layer for the coarser domain. A possible way to improve the quality of the simulations for this time period would be to proceed to observations assimilation. Satisfactory results have been obtained with the Japanese SPEED and WSPEEDI-II emergency

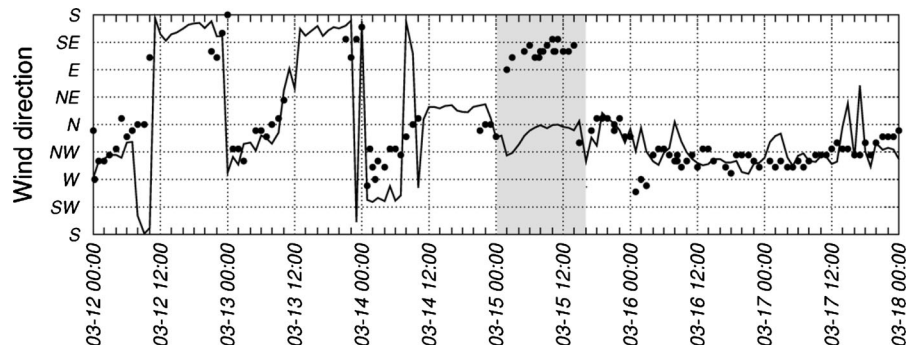


Figure 3

Wind directions observed at the METAR Fukushima airport station (black dots) and wind directions simulated using WRF (black solid line). The grey area corresponds to the period of time during which releases have been transported towards the northwest of Fukushima Dai-ichi plant

response systems (CHINO *et al.*, 2011; KATATA *et al.*, 2012a, b; TERADA *et al.*, 2012). Large-scale data used in these models have higher temporal and spatial resolution than the GFS ones and a large amount of local meteorological observations are assimilated. As our regional simulations are still ongoing, only long range results are presented in this article.

3.2. Long Range Simulations

Atmospheric Transport Modeling at global scale has been carried out using the particle dispersion lagrangian model FLEXPART (V.8.2) and the NCEP/GFS meteorological data (<http://weather.noaa.gov/pub/SL.us008001/ST.opnl>) with 6 h, $0.5^\circ \times 0.5^\circ$ and $1^\circ \times 1^\circ$ resolutions. This ATM system is suitable regarding the spatio-temporal characteristic scales of the problem to be solved. The objective of long range simulations is to assess the arrival time of radionuclides at different monitoring stations located over the globe and evaluate the quantities released into the atmosphere. As previously quoted, we will mainly focus on Xe-133 (half life 5.244 days), I-131 (8.023 days), and Cs-137 (30.05 years) which are volatile fission products (see Part I of the publication).

3.3. Gas and Particulate Deposition, Particle Size and Emission Height

During events such as the Fukushima or Chernobyl accidents, gases and particles emitted in the

atmosphere can be transported over very long distances and over long periods of time. Typically, the spatio-temporal scales of the problem are of the order of the circumference of the globe and several months. Because of these atmospheric dispersion and transportation scales, radioactive decay, gas-particulate conversion, and dry and wet deposition can drastically affect the behavior of emitted material. It should be noted that the noble gases (such as radioxenon) are not affected by deposition phenomena.

Wet deposition of gases or aerosols on the ground is due to the washout of the radionuclide plume by precipitation (rainfall, snow, etc.). It does not depend linearly on the precipitation rate. It is based on a scavenging coefficient, which depends on the precipitation rate and the considered radionuclide. To calculate the dry deposition of gases and aerosols, a classical approach in the dispersion models is to separate the gravity fallout (settling) and the interaction with soil and vegetation. The total deposition rate is the sum of these two contributions. The deposition due to interaction with the soil is calculated for altitudes between the ground and a reference height (e.g., 15 m). It is usually a function of aerodynamic drag terms produced by vegetation canopies and soil nature. Settling velocity is assumed to be zero for gases but depends on density and diameter for particles. This last point is important because as a FLEXPART particle can not represent several settling velocities, gases and aerosols trajectories must be calculated separately.

Preliminary calculations were performed to estimate the relative influence of particle size and deposition processes on the atmospheric transport efficiencies calculated at several IMS stations located in the northern hemisphere (see Appendix). By efficiency of atmospheric transport at a given point, we mean the activity concentration calculated with a unit release. Figure 4 (left) shows the normalized efficiencies calculated at the locations of 14 IMS stations. Efficiencies are normalized to the maximum reached at the station JPP38-Takasaki. Calculations are carried out with 1 and 0.1 μm particle diameters (KANEYASU *et al.*, 2012), respectively. The result shows that the variation of particle diameter in this range has a small influence on the calculated behaviour of particles in the flow. Figure 4 (centre) shows the efficiencies obtained by considering on the one hand an inert tracer (i.e., without wet and dry deposition) and an aerosol with 1 μm diameter and dry deposition on the other hand. As expected, dry deposition has a weak effect on submicronic particles during transport. Figure 4 (right) shows the efficiencies calculated by using both an inert tracer and a 1 μm diameter aerosol with wet and dry deposition. With precipitation rates included in employed GFS data, wet deposition appears to have a significant effect on the results.

The height at which the radionuclides are emitted can have a significant influence on their dispersion into the atmosphere. QIAO *et al.* (2011) used a climate model to estimate the long range dispersion of Fukushima releases over a period of 3 months. In

particular, they studied the influence of the emission height of radionuclides by selecting a release close to the ground, in the 5,000 m layer and the 10,000 m layer. Particles are transported more rapidly towards North America, Europe and Asia especially when their emission height is high. In our simulations, since the releases were not energetic (excluding cooling pool fires) and the explosions that occurred were controlled, it is considered that releases take place in the 0–200 m layer. As mentioned in the following section, radionuclides can quickly reach the middle and upper troposphere in situations when an updraft occurs.

4. Meteorological Conditions

Figure 5 shows the large-scale meteorological patterns for four dates between March 15 and March 24 (the maps were produced from NCEP/GFS 0.5° data using the GrADS system [<http://www.iges.org/grads/>]). These different patterns present wind vector fields and geopotential height at 500 hPa. Geopotential height is useful to highlight large-scale cyclonic and anticyclonic structures. During this time period, a strong westerly jet stream blew over the Pacific Ocean from Japan to California, and over the Atlantic Ocean from the North American continent to Iceland. The flow was then directed towards the north pole because of a high pressure system over Europe (e.g., March 15 map). The high pressure structure established over Western Europe then led the flow to Central Europe. Because the

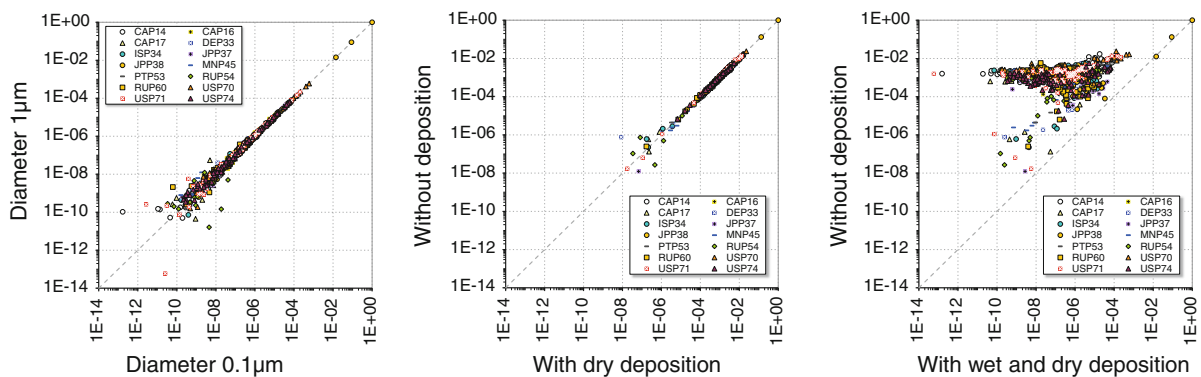


Figure 4

Left influence of particle diameter on transport efficiencies. Center influence of dry deposition. Right influence of wet deposition

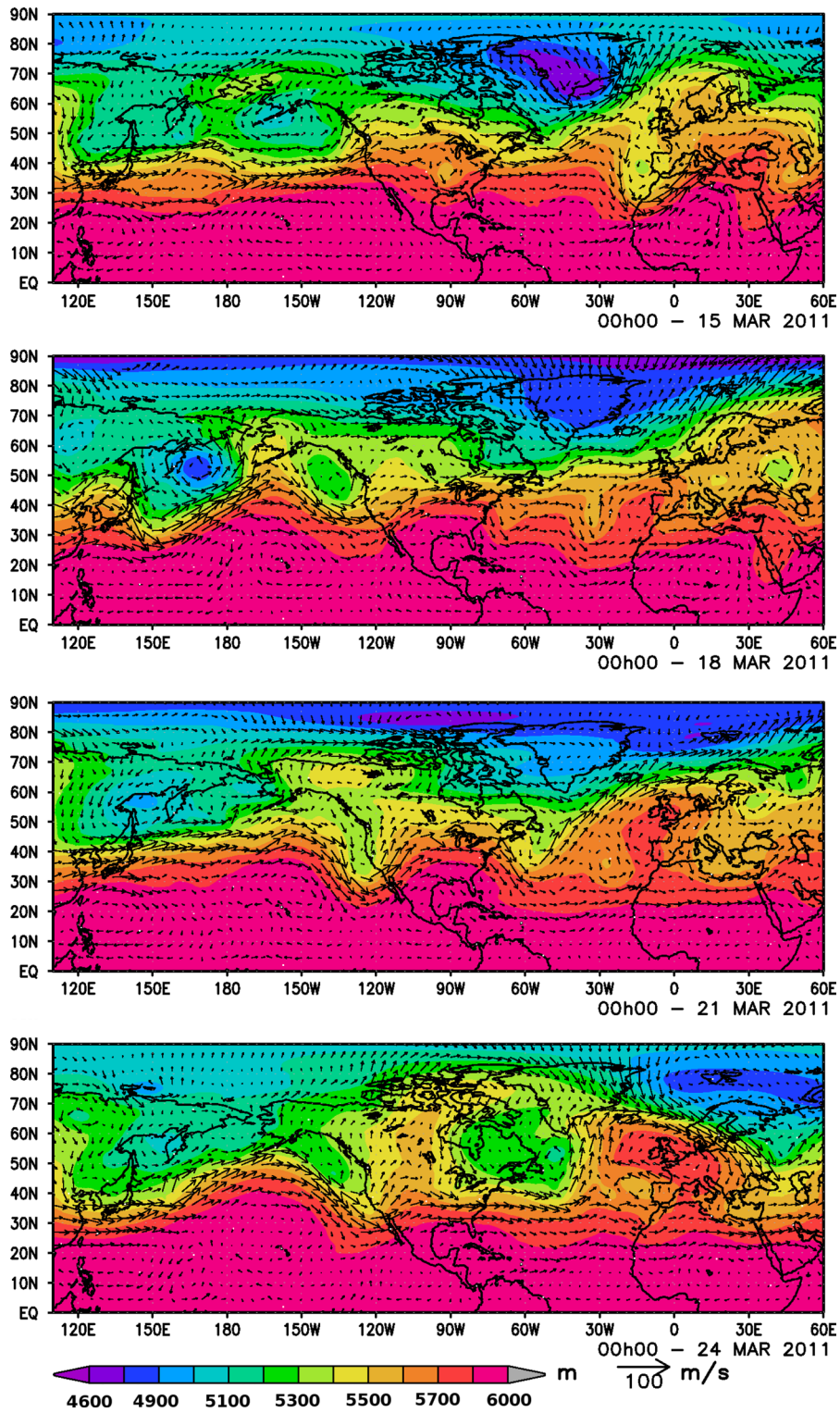


Figure 5
Large-scale wind field at 500 hPa (NCEP/GFS). Scale color geopotential height (m)

downdraft was located on Eastern Europe, radionuclides suspended in the atmosphere could have reached Eastern Europe before reaching Western Europe (e.g., March 21 and 24 maps). Radionuclides released into the atmosphere were rapidly transported around the globe, and achieved a circumnavigation in 2–3 weeks. TAKEMURA *et al.* (2011) indicate that a large-scale updraft caused by a low pressure system was located over Japan from March 14 to 15 at the time of the explosion of unit 2 (Table 1). This meteorological situation allowed radioactive particles present in the boundary layer to reach the middle and upper troposphere and the jet stream layer, and finally transported them over the Pacific Ocean in 3 or 4 days.

5. Radionuclides Considered in Dispersion Simulations

The analysis of the Chernobyl accident showed that large amounts of Cs-137 and especially of I-131 were emitted into the atmosphere (UNSCEAR, 2000). In order to compare these quantities with those released during the Fukushima accident, Cs-137 and I-131 are considered in the simulations. Because of the complexity of events that occur during such accidents, it is difficult to estimate what were the distributions of particle diameters and the gas/particulate ratios (I-131) that were emitted into the air. However, concerning long range simulations, it seems reasonable to assume that only small particles may be transported over such long distances. Without further information, a single 1 μm diameter particles distribution for Cs-137 and I-131 was considered. In addition to the Cs-137 and I-131, simulations were performed with Xe-133. Hence, as previously mentioned, in the framework of the Comprehensive Nuclear Test Ban Treaty (CTBT), monitoring of atmospheric concentration of radioxenon is relevant to provide evidence of atmospheric or underground nuclear weapon tests. However, during the couple of months after the Fukushima Dai-ichi accident, monitoring capabilities of the network could have been affected by the large amount of radioxenon released by the accident. The impact of Fukushima radioxenon releases on the worldwide Xe-133 background must also be investigated.

5.1. I-131

The gaseous form of I-131 is supposed to be deposited on the ground by the washout of the plume (wet deposition). CAPUT *et al.* (1993) have conducted experiments to determine the washout factor of elemental iodine in the gas form. The results show that molecular gaseous iodine, which is very reactive, seems to be irreversibly captured in rainwater. The average washout factor determined from experiments is $\Lambda = 8.2 \times 10^{-5} \text{ s}^{-1}$ (this coefficient indicates the fraction of radioisotopes washed out from 1 m^3 of air per second at a standard rain intensity of 1 mm h^{-1}). This value is of the order of magnitude of those generally accepted in deposition models [e.g., $\Lambda = 7 \times 10^{-5} \text{ s}^{-1}$ (PITTAUEROVÁ *et al.*, 2011)]. In the FLEXPART model, gaseous I-131 washout factor is set to $\Lambda = 8 \times 10^{-5} \text{ I}^{0.62} \text{ s}^{-1}$, where I is the intensity of the rain in mm h^{-1} . Scavenging factor for particulates of I-131 is given by $\Lambda = 1 \times 10^{-4} \text{ I}^{0.8} \text{ s}^{-1}$. The dry deposition velocity of gaseous I-131 is calculated using the resistance method (WESELY and HICKS, 1977). Calculated deposition velocities (interaction with soil) are approximately in the range 1×10^{-3} – $1 \times 10^{-2} \text{ m s}^{-1}$. These values are consistent with those generally accepted in impact assessment models (BIOMASS program, 2003). For the I-131 aerosol form, considering a 1 μm particle diameter class, the dry deposition velocity is of the order of $1 \times 10^{-4} \text{ m s}^{-1}$. This value is one order of magnitude smaller than those currently used in particle deposition models with diameters above 1 μm (about $1 \times 10^{-3} \text{ m s}^{-1}$) (BIOMASS program, 2003). In the case of particle diameters above 1 μm , the deposition velocity is increased by gravity settling (SLINN, 1982; SEHMEL, 1980). Radioactive decay of I-131 is taken into account in the simulations.

5.2. Cs-137

The below cloud scavenging factor for Cs-137 is given by $\Lambda = 1 \times 10^{-4} \text{ I}^{0.8} \text{ s}^{-1}$. The calculated dry deposition velocity is about $1 \times 10^{-4} \text{ m s}^{-1}$ when considering 1 μm diameter particles. Regarding the simulated durations (several weeks), the influence of radioactive decay of Cs-137 will be negligible on calculated activity concentrations.

5.3. Xe-133

Radionuclides are highly volatile fission products. Noble gases are not affected by wet and dry processes. Radioactive decay of Xe-133 is taken into account in the simulations.

5.4. Iodine Gas/Particle Conversion

The behavior of I-131 in the atmosphere is known to be complex as the gaseous form could gradually evolve into the particulate form. This has been the subject of many studies, particularly following the accident at the Chernobyl plant in April 1986. UEMATSU *et al.* (1988) used atmospheric measurements made in Japan and on a boat in the Pacific Ocean to estimate the characteristic conversion gas/aerosol time for I-131. With the assumption that about 60 % of the total I-131 was present in the gas form in the Chernobyl releases, they found an average conversion time of about 2–3 weeks, with a minimum conversion time of about 12 days. The relative uncertainty is estimated to be about a factor of 2. MASSON *et al.* (2011) indicate that the I-131 gas/I-131 total (total = gas + particles) ratio measured at the site of the Fukushima Dai-ichi plant from March 22 to April 4, 2011 was 71 ± 11 %. The average ratio measured in Europe until April 12 on a station network is very close, 77 ± 14 %. According to the authors, the similarity of the measured ratios suggests that the conversion gas/particle is small.

To verify this hypothesis, a calculation of atmospheric dispersion was performed by considering a single release which occurred on March 14 from 18 to 24 h (UTC), linked to the explosion on unit 2. In this numerical experiment, the release is assumed to be made up of 70 % of I-131 gas and 30 % of I-131 aerosol and a diameter of 1 μm is chosen for particulate form. The wet and dry deposition processes for gas and particulate forms are those described above. The radioactive decay of I-131 is taken into account, but gas/particle form transfers are not simulated. Assuming that the deposition process is realistically reproduced, the transfer between the gas phase and particulate phase can be considered low if the gas/particle ratio calculated in Europe is close to the initial release one.

Figure 6 (left) presents the activity concentrations obtained at some IMS stations located in Western Europe. The radionuclides released into the atmosphere during the simulated event reached monitoring stations between March 24 and April 13, which is in good agreement with measurements carried out in Europe (MASSON *et al.*, 2011). The figure shows that travel time is about 2–4 weeks. Figure 6 (right) shows the simulated gaseous I-131/total I-131 ratios. Considering that the maximum simulated activity concentration is about $4,000 \mu\text{Bq m}^{-3}$ and assuming a detection limit of $0.5 \mu\text{Bq m}^{-3}$, the average simulated gaseous I-131/total I-131 ratio is about 94 % (95 % considering all the values calculated without taking the detection limit into account). This result may indicate that about 40 % of gaseous I-131 should be converted to particulate phase to match the measured average ratio in Europe ($\sim 77 \pm 14$ %). According to the travel time between Japan and Europe, this suggests that the conversion time is in good agreement with the one proposed by UEMATSU *et al.* (1988). However, due to the uncertainties of the simulations and measurements, this work should be continued. Iodine gas/particle conversion is not taken into account in the simulations.

6. Simulations at the JPP38: Takasaki Station

Simulations are carried out using NCEP/GFS global meteorological data with 6 h and 0.5° resolution. Figure 7 shows the activity concentrations calculated at the JPP38 station (see Appendix, Fig. 17) selecting the releases from Table 1. The activity concentrations are normalized to the total. For each event, it is assumed that the release lasts 2 h and that a unit amount of an inert tracer is emitted (without deposition or radioactive decrease). A short duration release is chosen to distinguish the relative contribution of each emission at the monitoring station.

6.1. Cs-137

Due to the relatively short distance between Fukushima Dai-ichi and JPP38 (~ 210 km), it was considered that the behavior of a tracer can be representative of the behavior of small sized aerosols

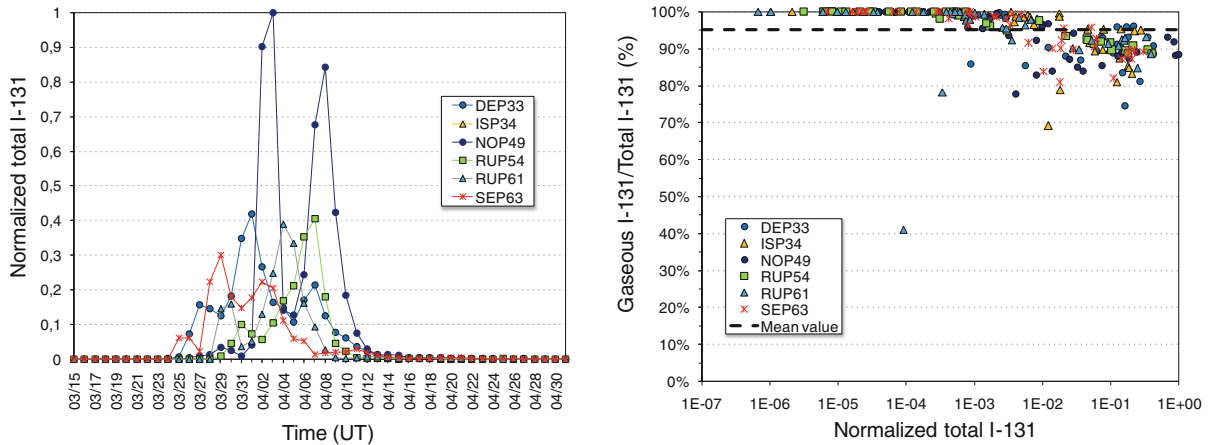


Figure 6

Estimation of iodine gas/particle conversion. *Left* activity concentrations calculated at the location of IMS stations situated in western Europe. *Right* corresponding gaseous/total I-131 ratios

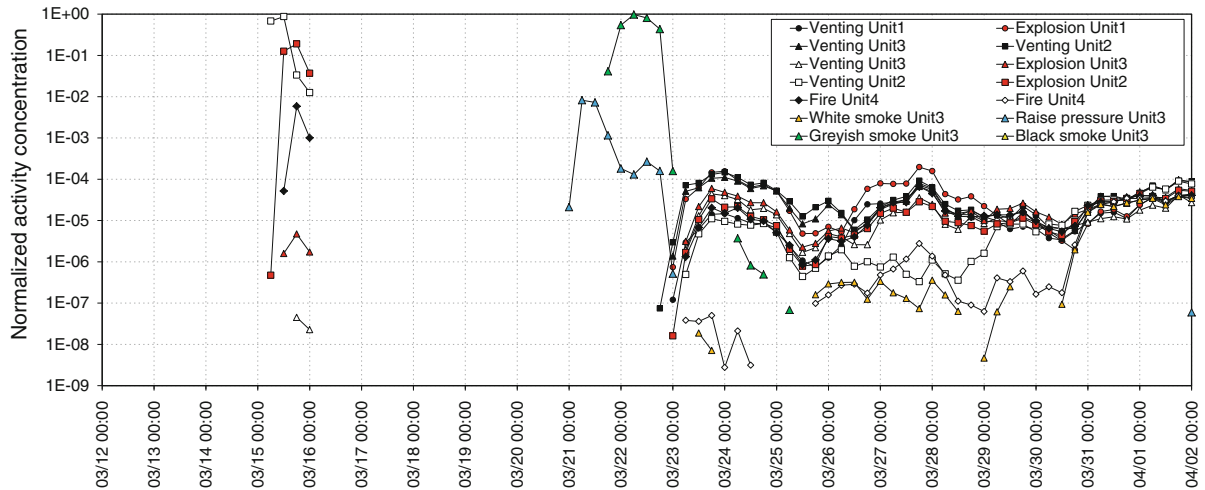


Figure 7

Calculated normalized activity concentrations at the JPP38 Takasaki station considering main events identified in Table 1

of Cs-137 during the first few days of the accident. Results presented above have shown that the behavior of aerosols was insensitive to the particle diameter when it was smaller than $1 \mu\text{m}$ (Fig. 4). For this particle size, it was shown that dry deposition phenomena were weak. Previous results also highlight that wet deposition was not very effective for the period leading to higher activity concentrations of JPP38. Figure 7 shows that the calculated activity concentrations were almost the same on March 15 and for the period from March 21 to 23. During those days, the northeasterly wind was favorable to the transport of radionuclides towards the station. The figure shows

that on March 15, the station was mainly sensitive to releases 7 and 8 (venting and explosion of unit 2) that occurred in the late afternoon of March 14. For the March 21 to 23 period, the station was sensitive to releases 12 and 13 (rise of primary containment vessel pressure and greyish smoke on unit 3) that occurred during March 20 and 21. From March 23, the contribution of other releases is more difficult to assess. From March 30, radionuclides emitted at the beginning of the event were able to travel around the globe and to contribute to the simulated signal.

Figure 8 (left) presents the activity concentrations calculated and observed at JPP38 station for Cs-137.

The activity concentrations calculated are those obtained by considering a continuous release from March 12 to April 1, 2011 and also the total contribution of all short releases (Fig. 7). The release rate is the same in all simulations. Results are normalized by the maximum activity concentration calculated for the period, obtained with the continuous release. The measured activity concentrations are normalized by the maximum observed, reached on March 15, 2011. The dynamics of the measurements is relatively well reproduced by the simulations. On March 15 and for the period from March 21 to 23, the activity concentrations from the simulated puffs and continuous release are substantially equivalent. This indicates that during these days, releases that occurred on late March 14 and during March 20 and 21 have mainly contributed to the measured signal. However, the figure shows significant activity concentrations measured on March 31, which are only reproduced with the continuous release scenario. Differences observed between the continuous release and puffs may reflect the fact that releases which have reached JPP38 may have lasted more than 2 h. This also points out that other events than those identified in Table 1 may have occurred. Figure 8 (right) shows the comparison between measured and simulated activity concentrations. On March 15, a reasonable agreement is obtained by considering a total release of the order of $\sim 5 \times 10^{16}$ Bq on March 14 (releases 7 and 8). For March 21 to 23, a fairly good agreement is found by considering a release of the order of $\sim 2 \times 10^{16}$ Bq on March 20 (release 12) or $\sim 4 \times 10^{14}$ Bq on March 21 (release 13). The total estimated release of Cs - 137 is of the order of 5×10^{16} – 7×10^{16} Bq.

In Fig. 8 (right), an additional release of $\sim 3 \times 10^{14}$ Bq was added during March 29 in order to reproduce the observed peak during March 30 and 31. In order to determine the effective release period, a backward calculation was carried out from the monitoring station for those 2 days (Fig. 9, left). Measurements of dose rate on the monitoring points located close to the Fukushima Dai-ichi NPP show a rise of the signal over March 28 and 29 (Fig. 9, right). These observations are in agreement with the hypothesis that an atmospheric release may have occurred during these dates. However, no particular

event has been identified in news reports concerning the accident (NISA). CHINO *et al.* (2011) have made an estimation of the I-131 and Cs-137 source terms released into the atmosphere between March 12 and early June 2011. To satisfy the agreement between simulation and measurements, the authors have found that an increase of 1.4×10^{14} Bq h⁻¹ in Cs-137 was needed between March 29 and 30.

6.2. I-131

Figure 10 (left) presents the activity concentrations calculated and observed at JPP38 station for I-131. The calculation of the dispersion takes into account the radioactive decay of I-131. It was assumed that fires that occurred on unit 4 cooling pools could not lead to I-131 releases as the unit had already been stopped at the time of the tsunami and the spent fuel was too old to release appreciable amount of I-131. As for Cs-137, aerosols are assumed to be small enough to behave as a gas and to neglect the dry deposition phenomena. It was also assumed that wet deposition is not effective for periods during which the main peaks have been measured. Because of the short transport time between the release point and monitoring stations (distance ~ 210 km), the gas/particle conversion have been neglected. By considering that the measurements at the IMS stations are only representative of the contribution of aerosols, a correction coefficient has to be applied to account for the fact that I-131 releases are also composed of gas. For aerosols, quite good agreement is obtained by considering a total release of the order of 6×10^{17} Bq at the end of the day on March 14 (releases 7 and 8: venting and explosion on unit 2). From March 21 to 23, an agreement is found by considering a release of the order of $\sim 4 \times 10^{16}$ Bq on March 20 (release 12) or $\sim 4 \times 10^{14}$ Bq during March 21 (release 13). An additional release of $\sim 2 \times 10^{14}$ Bq was added during March 29 to match the observed peak during the March 30 and 31 period. An increase in I-131 release rate was also needed between March 29 and 30 in CHINO *et al.* (1.8×10^{14} Bq h⁻¹). The estimated total release is about $\sim 6 \times 10^{17}$ Bq. Assuming that the initial releases composition was 70 % gas and 30 % particles, the total I-131 estimated release is found to be $\sim 2 \times 10^{18}$ Bq.

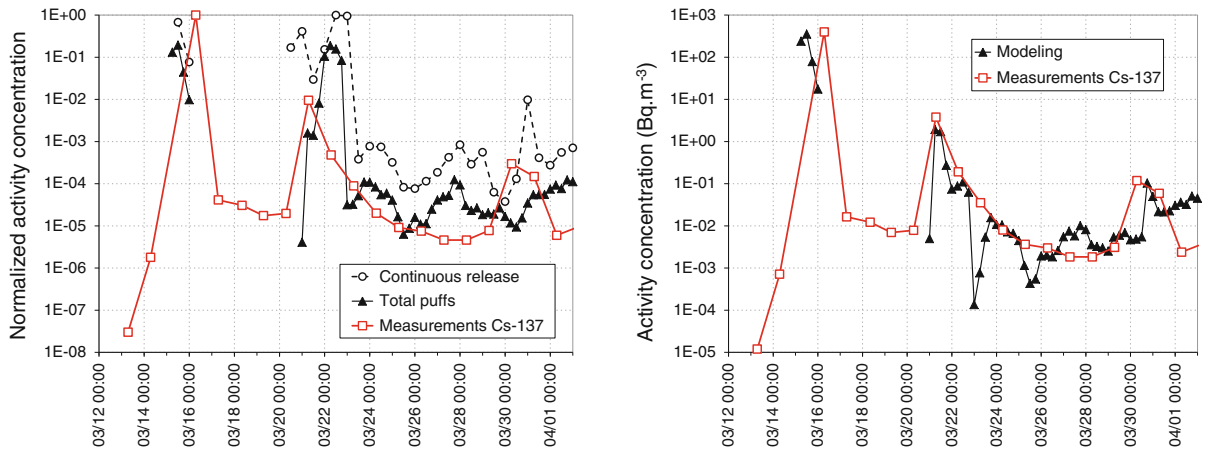


Figure 8

Left normalized Cs-137 activity concentrations measured and calculated at the JPP38 Takasaki station considering a continuous release and main identified events. *Right* Cs-137 activity concentrations measured and simulated using estimated source terms

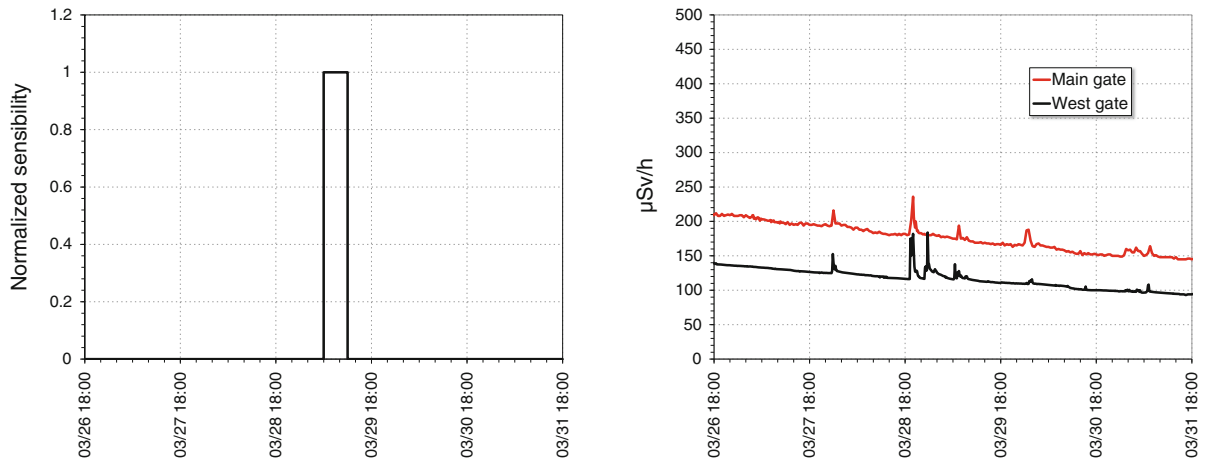


Figure 9

Left sensitivity between the site of Fukushima Dai-ichi site and the JPP38 station for a backward calculation started on March 30 and 31 from the station. *Right* dose rates measured on the monitoring points Main Gate and West Gate between March 26 and 31

Other releases, which have not reached the monitoring station due to meteorological conditions, might have to be added to the estimated I-131 and Cs-137 releases. Uncertainties on calculated source terms are significant and are related in part to the measurements. The I-131 and Cs-137 uncertainties have been assessed at $\pm 25\%$ ($3,700 \pm 1,000 \text{ Bq m}^{-3}$ and $400 \pm 100 \text{ Bq m}^{-3}$, respectively) on March 15 measurements. In addition, after March 15, the JPP38 radionuclide station had been contaminated by the radioactive cloud as shown in Part I of the publication. Uncertainties on source terms are also related to inaccuracies in the wind fields used and may also be due to the

dispersion model itself. Hence, the 0.5° wind fields may not be sufficiently resolved to match the JPP38 observations, as this station is close to Fukushima and located in an area where the topography is complex (Appendix, Fig. 17).

7. Evaluation of Source Terms with Long Range Simulations

Atmospheric transport of aerosols was carried out using 1.0° NCEP/GFS data and simulations related to the Xe-133 were performed with 0.5° data. To

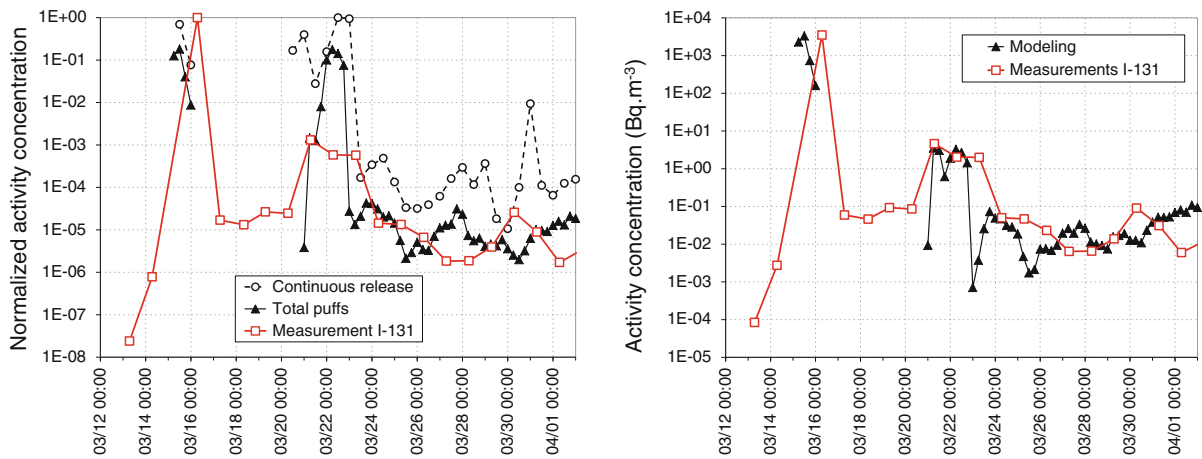


Figure 10

Left normalized I-131 activity concentrations measured and calculated at the JPP38 Takasaki station considering a continuous release and main identified events. Right I-131 activity concentrations measured and simulated using estimated source terms

assess the influence of the wind fields resolution on long range simulations, a calculation was performed by simulating the dispersion of an inert tracer continuous release emitted from the Fukushima Dai-ichi site during the period of time from March 12 to May 1, 2011. Calculations were performed with both the 1.0° and the 0.5° data. Figure 11 shows the results at several IMS stations located over the Northern hemisphere (see Appendix, Fig. 18). FA2 and FA5 bands are plotted in the figure to identify the 1.0° results which are in a factor of 2 or 5, respectively, compared to the results obtained at 0.5°. The two simulations appear to be in proper agreement, with FA2 = 87 % and FA5 = 97 %. The worst scores were obtained for the JPP38 station which is the closest to the Fukushima NPP. In this particular case, given the relative short distance between JPP38 and the facility, a better agreement between observations and simulations is obtained as expected with the 0.5° resolution data. For other IMS stations located at a longer distance from Fukushima, 1.0° and 0.5° wind fields are found to lead to substantially similar results.

Based on source terms evaluated from JPP38 station measurements, long range simulations were performed using 1.0° GFS wind fields. Direct calculations were carried out considering the events listed in Table 1. It is assumed that all events can lead to Cs-137 releases. As unit 4 was already shutdown at the time of the tsunami, it is assumed that the reactor

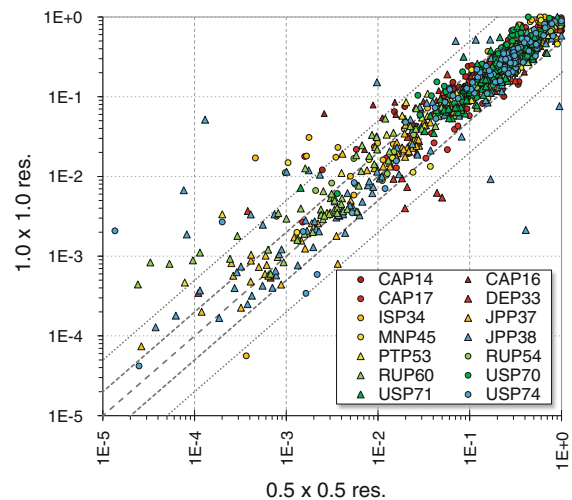


Figure 11

Comparison of activity concentrations simulated on IMS stations using 1.0° and 0.5° resolution GFS wind fields

and spent fuel cooling pools can not lead to I-131 releases. Because Xe-133 is highly volatile, it is considered to be emitted into the atmosphere at the time of the hydrogen explosions of units 1, 2 and 3.

All simulations indicate that the material emitted into the atmosphere mostly remained over the northern hemisphere, showing that the inter-hemisphere exchanges are limited. Only a few minor detections were observed over the southern hemisphere (e.g., for I-131: 1 μBq m⁻³ at FJP26, Nadi,

Fidji, from April 5 to 6 and $7 \mu\text{Bq m}^{-3}$ at PGP51, Kavieng, Papua New Guinea, from April 11 to 12).

7.1. Cs-137

Figure 12 shows the evolution of observed and simulated Cs-137 activity concentrations. Temporal synchronization between observations and simulations is satisfactory. From one station to another, relative activity concentration level differences are not only based on the distance travelled by the plume from Japan (for readability of the figures, the y axis may be different). For example, the simulated and observed levels at the MNP45 station (Ulaanbataar, Mongolia) are higher than those obtained at the DEP33 station (Freiburg, Germany). This indicates that the complex transport of radionuclides in the atmosphere has been, in part, well reproduced in the simulations. However, long range transport of Cs-137 aerosols appears difficult to simulate. Hence, poorer results have been obtained for stations located on the edge of the simulated plume and/or close to Fukushima plant. This is particularly the case for RUP60 station (Petropavlovsk, Russia), which is located about 2,200 km northeast from Fukushima and for USP71 (Sand Point, USA) and CAP16 (Yellowknife, Canada) stations located at 62.5N and 55.33N respectively. Bias on transport of Cs-137 may be due to the cumulative effect over long distances of wind fields inaccuracies and/or an underestimation of the dispersion of lagrangian particles with high latitudes. Depending on the intensity of precipitation rates contained in the meteorological input data, the wet deposition can also be locally overestimated or underestimated on the path of the particle cloud. Uncertainties on the initial size distribution of aerosols can also affect the representativeness of the calculated dry deposition. Some of the differences between simulations and observations may also be due to specific phenomena that have not been taken into account, such as re-suspension of part of cesium initially deposited on the ground. Some smaller peaks observed after the main peaks may be due to the resuspension.

At stations where the aerosol behaviour is the most consistent with the observations, the source terms evaluated using the JPP38 detections lead to an

overestimation of the long distance simulated detections. Total release estimated from the long range simulations is about 1×10^{16} Bq (~ 5 – 7 times lower than those obtained using the JPP38 measurements). The simulations show that the events that occurred in the afternoon of March 14 UTC on the unit 2 may have led to significant releases of Cs-137 in the atmosphere. For these events, a total release of the order of 6×10^{15} Bq is required to find an agreement with the measurements (~ 10 times lower than for the JPP38 calculation). The events on the unit 3 and that took place from March 20 to 23 are also found to be significant with a required total release of the order of 2×10^{15} Bq. Simulations suggest that the hydrogen explosion and/or venting operations of units 1 and 3 (March 12 and 13/14) may have resulted in a total release of 2×10^{15} Bq.

7.2. I-131

Figure 13 shows the evolution of observed and simulated I-131 activity concentrations. To perform the comparison at the IMS stations, simulations were carried out considering only the aerosol fraction of emissions (iodine gas phase is not measured by IMS stations). The agreement between simulations and observations is generally better for I-131 than for Cs-137. This can be attributed to the half-life of I-131 (8.023 days), which leads to a faster depletion of the cloud and thus reduces the relative errors of simulations (due to wet deposition, etc.). The dynamics of the measurements is rather well reproduced by the simulations (note that the amplitude of the y axis of USP70 and USP71 stations is different from the other stations). The temporal synchronization between observations and simulations is quite satisfactory. As for the Cs-137, poorer results are obtained for stations located on the edge of the simulated plume and/or near Fukushima: e.g., RUP60 (Petropavlovsk, Russia), CAP16 (Yellowknife, Canada) and USP71 (Sand Point, USA) stations. A general agreement is nevertheless obtained by considering a total I-131 aerosol source term of approximately 1×10^{17} Bq emitted during the different puffs. Assuming that the I-131 aerosol release represents only 30 % of the total emission, the total release (aerosol + gas) would be about 4×10^{17} Bq without considering

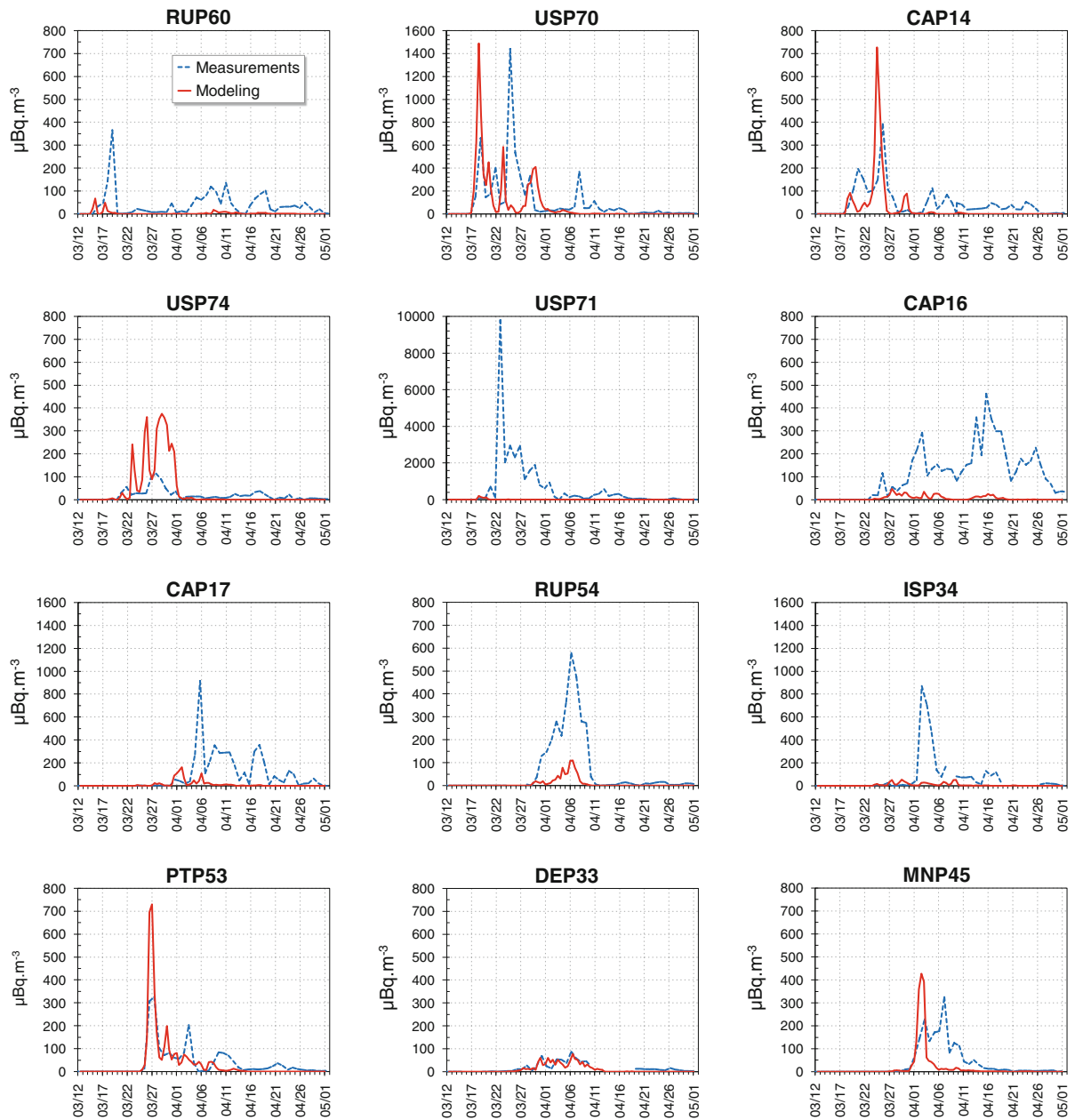


Figure 12

Activity concentrations in Cs-137 measured and simulated from March 12 to May 1, 2011 at some IMS stations. The stations are represented according to the dates of arrival of the plume of radionuclides. *Top left* the station that detected the earliest. *Bottom right* the station that detected the latest

the gas/particle conversion phenomena. As for the Cs-137, a factor ~ 5 is observed between the estimated total releases from simulations at JPP38 and distant stations. Simulations show that the events which took place in the afternoon of March 14 UTC

on the unit 2 led to major releases of I-131 in the atmosphere. For these events, a release of the order of 6×10^{16} Bq is required to find an agreement with measurements (~ 10 times lower than for the JPP38 calculation). Events on unit 3, which took place from

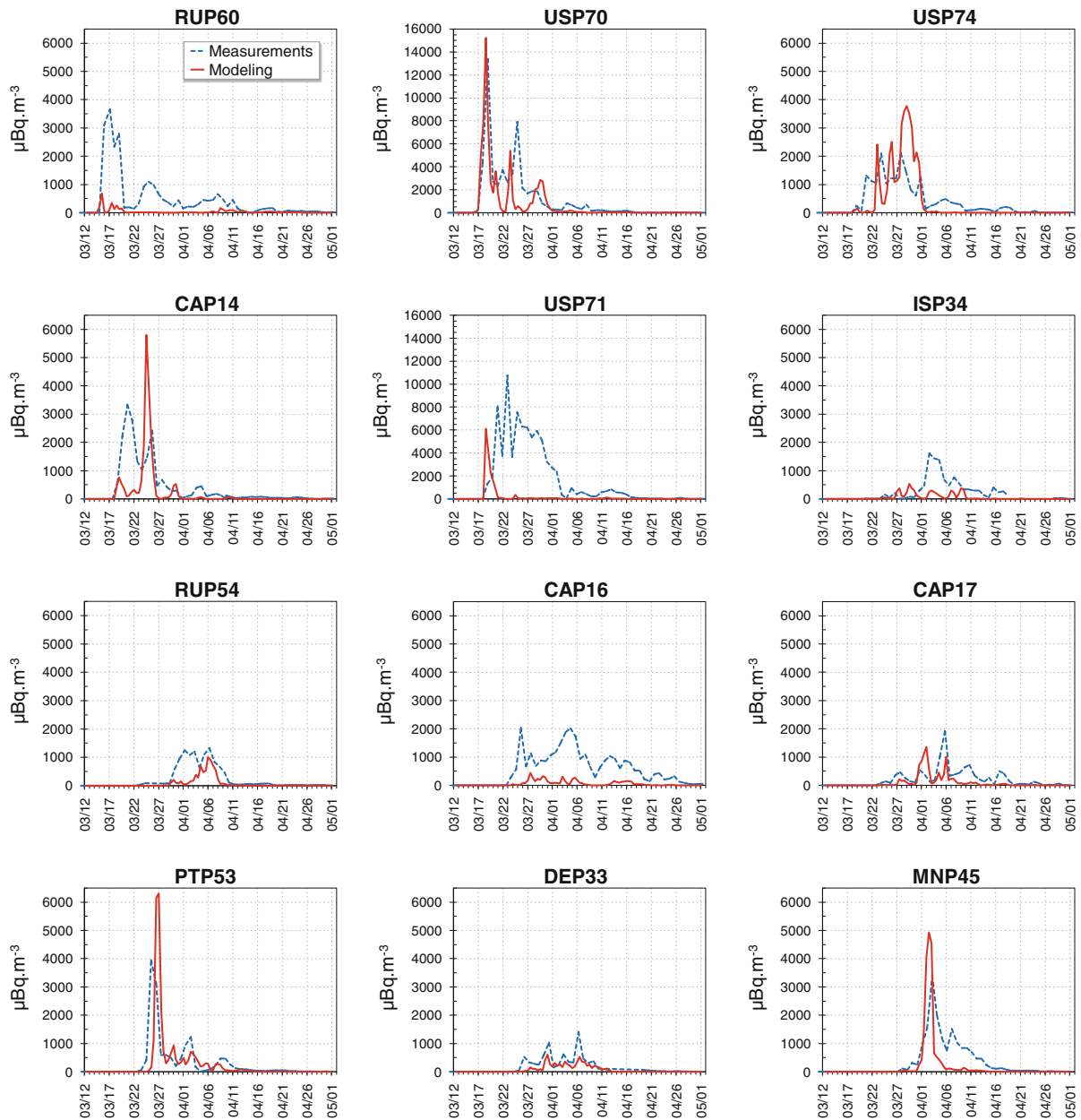


Figure 13

I-131 activity concentrations measured and simulated from March 12 to May 1, 2011 at some IMS stations. The stations are represented according to the arrival dates of the plume

March 20 to 23, are also found to be significant, with a required release of the order of 3×10^{16} Bq. For example, the 1.4 mBq m^{-3} peak measured from the April 5 to 6 UTC at DEP33 station (Freiburg, Germany) seems to be correlated with these emissions. Simulations show that the venting and

hydrogen explosion related to unit 1 (March 12) may have led to significant releases of about 2×10^{16} Bq. Simulations suggest that the peak of 13.4 mBq m^{-3} measured from March 17 to 18 UTC by the USP70 (Sacramento, USA) station could be mainly due to these releases.

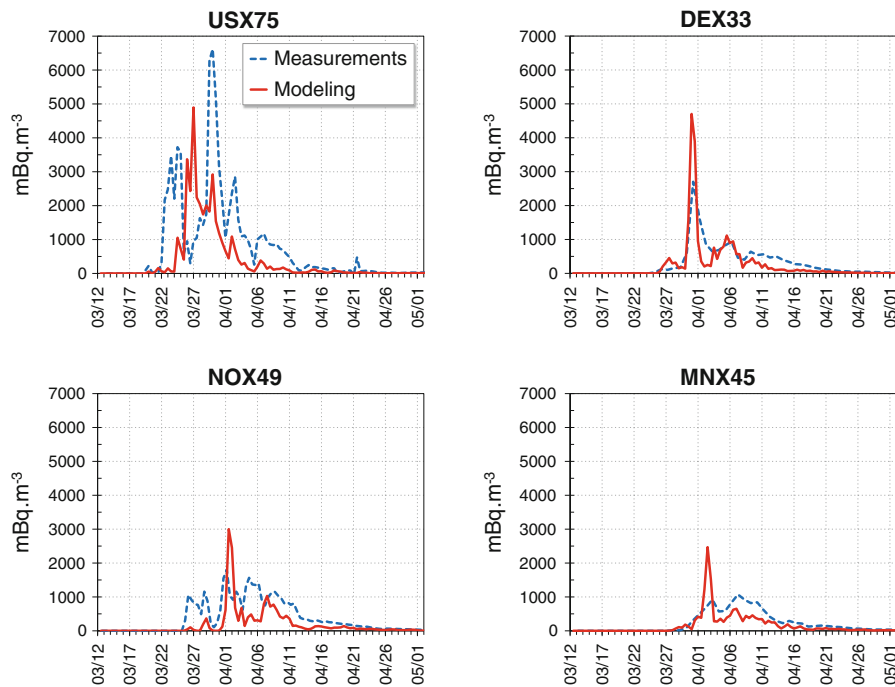


Figure 14

Activity concentrations in Xe-133 measured and simulated from March 12 to May 1, 2011 at some IMS stations. The stations are represented according to the dates of arrival of the plume

7.3. Discussion on Cs-137 and I-131 Results

Releases calculated for Cs-137 and I-131 appear to be much larger than those calculated for the continuous leakage between March 22 and mid-May 2011 (see Sect. 2.2). Continuous leakage calculated from March 22 may represent only 1/100 (Cs-137) and 1/1,000 (I-131) of total releases and they will be neglected.

Total source terms calculated from long range simulations for Cs-137 and I-131 (resp. 1×10^{16} Bq and 1×10^{17} to 4×10^{17} Bq) are in good agreement with those presented in the literature (CHINO *et al.*, 2011; MATHIEU *et al.*, 2012; WINIAREK, 2012) These results suggest that the source terms estimated from the station JPP38 are probably too high. CHINO *et al.* (2011) found also that the largest releases took place on early March 15 and that no major release occurred after March 24 which is also consistent with our results. The main releases could be linked to the explosion and the pressure suppression chamber damage of unit 2. However, our simulations suggest that the hydrogen explosions and/or venting

operations of units 1 and 3 (March 12 and 13/14) may have also resulted in significant releases (KATATA, 2012a). Because of the meteorological situation, these releases seem to have been rapidly blown towards the Pacific Ocean (especially the release of March 12) and may not have been significantly measured by the stations network in the vicinity of the NPP.

It was estimated that the total Cs-137 and I-131 releases emitted into the atmosphere during the Chernobyl accident were 8.5×10^{16} and 1.8×10^{18} Bq respectively. Concerning this event, the release of Cs-137 was estimated to be about 30 % of the core inventory and that of I-131 is estimated to be about 50 % (UNSCEAR). The source terms estimated in our study from long range simulations show that Fukushima releases could represent about 10 % of the Chernobyl emissions for these two isotopes.

7.4. Xe-133

Because of its high volatility, it is estimated that the Xe-133 was mainly emitted into the atmosphere

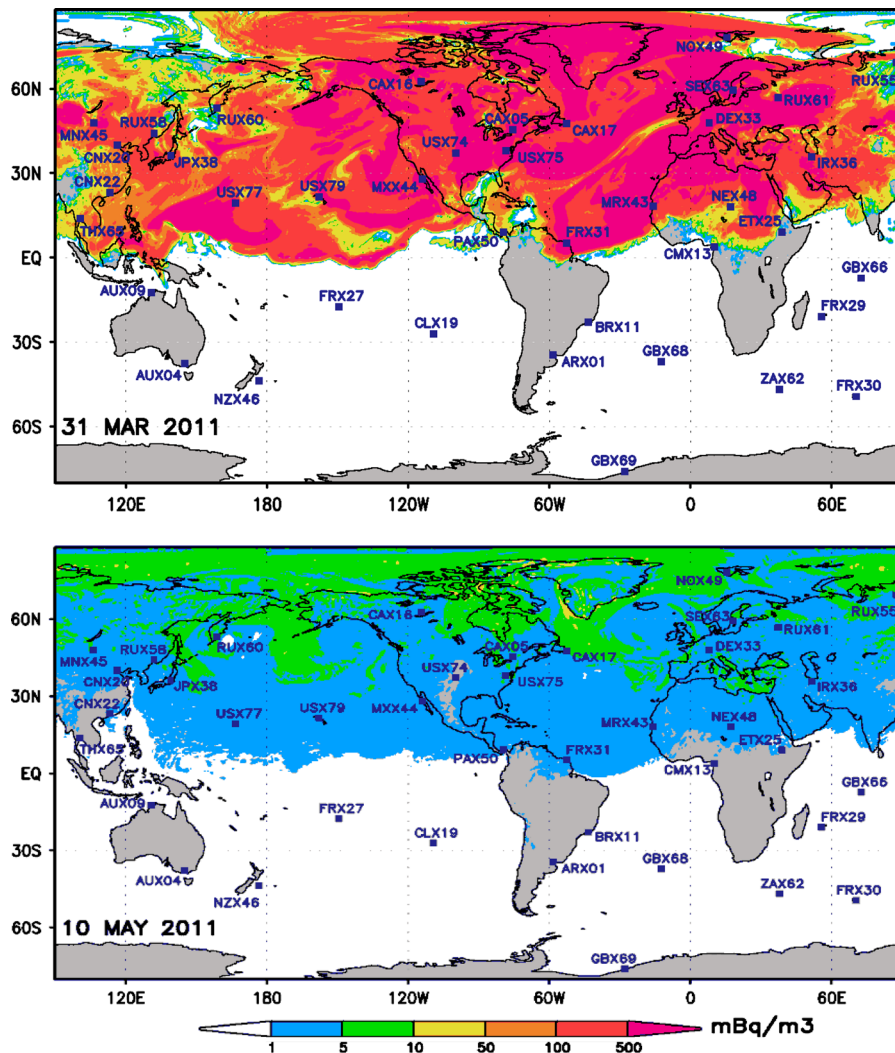


Figure 15

Xe-133 activity concentrations at ground-level for two dates. All IMS noble gas stations are represented on the maps

during the hydrogen explosions of units 1, 2 and 3. Releases are supposed to have occurred over 6 h time periods centered at the time of explosions, which allows us to consider some venting and leakage before and after those moments. Figure 14 shows the activity concentrations (expressed in mBq m^{-3}) measured and calculated at some IMS stations located in the northern hemisphere (see Appendix, Fig. 19). Quite good agreement is obtained considering that $\sim 2 \times 10^{18}$ Bq are released during each puff (total release of $\sim 6 \times 10^{18}$ Bq).

As previously observed, the results are less satisfactory at stations located on the edge of the

simulated plume. For other stations, a fairly good temporal synchronization is obtained and the dynamics of the measurements is globally well reproduced. Figure 15 shows the maps of calculated activity concentrations for two selected dates within a 2 month period after the beginning of the releases. Results show that the cloud was dispersed in the whole northern hemisphere and as mentioned previously, that air exchanges between north and south were low (as for the Chernobyl event). The maps suggest a relatively rapid decrease of concentrations, resulting from the dispersion of gas and half-life of Xe-133. Because of the large amount of radioxenon

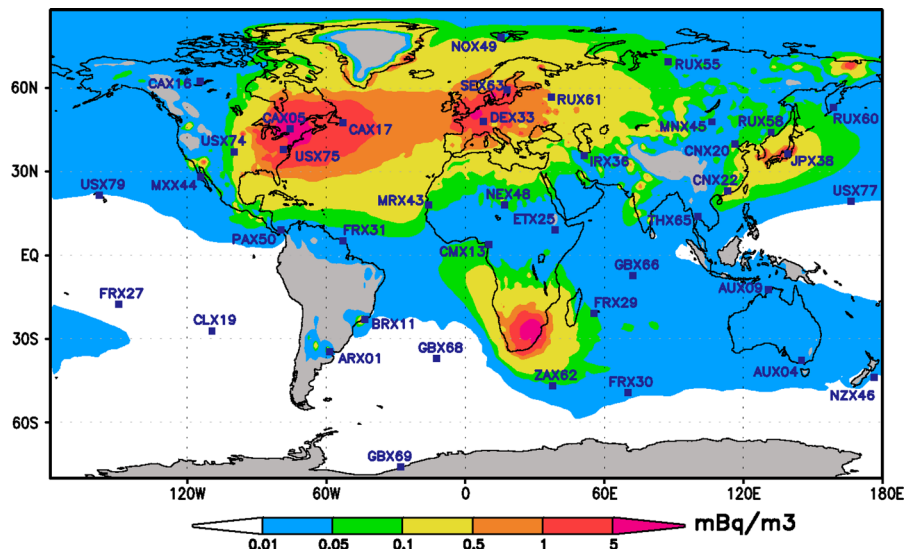


Figure 16

Global average simulated background in Xe-133 due to atmospheric releases of major nuclear facilities during normal operation (ACHIM *et al.*, 2011): Nuclear Power Plants and factories producing radionuclides for medical use (MATTHEWS, 2010; KALINOWSKI and TUMA, 2009). These facilities are mainly distributed in the northern hemisphere (note that Figs. 16 and 17 color scales are different)

emitted into the atmosphere, high levels of activity concentrations were found that remained locally above 1 Bq m^{-3} for several weeks after the accident. Until early May, levels of activity concentrations remained significant throughout the northern hemisphere. They were above average levels usually observed due to releases of major nuclear facilities during normal operations (Fig. 16). From early May 2011, Xe-133 concentrations due to Fukushima Dai-ichi releases were of the order of magnitude of industrial background. Measurements show that the situation has returned to near normal since June. Xe-131 m/Xe-133 ratios measured over time by the CTBT noble gas network and French national devices show a clear signature of the Fukushima Dai-ichi accident over a long period of time (about 80 days). This information is useful to assess the monitoring capabilities of the network if another significant event occurred within a few weeks after the accident. For example, the USX75 station (Charlottesville, USA) has shown, 2 months after the accident, a typical signature from the Chalk River medical isotope production plant (Canada) that clearly exceeded the Fukushima ratios (see Part I of the publication).

The total estimated source term gives a fraction of core inventory of about $8 \times 10^{18} \text{ Bq}$ at the time of

reactor shutdown. This result suggests that at least 80 % of the core inventory has been released into the atmosphere and indicates a broad meltdown of reactor core (see Part I of the publication). Total source term is in good agreement with literature (MATHIEU *et al.*, 2012). However our result is lower than in STOHL *et al.* (2012) where the authors found a total release from 12×10^{18} to $18 \times 10^{18} \text{ Bq}$ which is higher than the entire estimated Xe-133 inventory. According to the authors, a significant part of Xe-133 released could be due to I-133 decay.

8. Conclusion

This part of the publication (Part II) is dedicated to atmospheric transport modeling. Simulations were mainly carried out at global scale by considering Cs-137, I-131 and Xe-133 volatile fission products to assess the arrival time of radionuclides at different IMS stations located on the globe and to evaluate the quantities released into the atmosphere. These analyses are valuable to estimate the Fukushima reactor core damages (Part I of the publication) and to assess the monitoring capabilities of the CTBT network following the accident.

All simulations show that the cloud has been mainly dispersed in the northern hemisphere and air exchanges appear to be very low with the southern hemisphere. Regarding Xe-133, the total release is estimated to be of the order of 6×10^{18} Bq emitted during the explosions on units 1, 2 and 3. This result suggests that at least 80 % of the core inventory has been released into the atmosphere and indicates a broad meltdown of reactor core. Due to the large amount of radionuclides emitted into the atmosphere, levels of activity concentrations remained locally above 1 Bq m^{-3} for several weeks after the accident. Until early May, levels of activity concentrations remained significant throughout the whole northern hemisphere. Xe-133 concentrations due to the Fukushima Dai-ichi accident decreased following the half life of the radionuclide to be of the order of magnitude of industrial background from mid May 2011. Measurements by noble gas stations located in the northern hemisphere show that the situation had returned to near normal during June 2011. The evolution of measured Xe-131 m/Xe-133 ratios shows a clear signature of the Fukushima Dai-ichi accident over a long period of time (about 80 days). The knowledge of activity concentrations and of isotopic ratios over time were essential to maintain the monitoring capabilities of the CTBT network if another major event had arisen in the weeks following the accident.

Regarding Cs-137 and I-131, simulations were performed considering both JPP38 and distant IMS stations measurements. Atmospheric transport modeling results are in a reasonable agreement with measurements on most stations but appear poorer for stations located on the edge of the simulated plume and/or close to Fukushima NPP. Bias on transport may be due to the considered source terms and to the cumulative effect over long distances of inaccuracies in wind fields. Calculations suggest that the main air emissions have occurred on March 14 (explosion and pressure suppression chamber damage of unit 2) and that no major release occurred after March 23. The JPP38 station appeared to be mainly concerned by March 14 and March 20 and 21 releases (rise of pressure of unit 3). The hydrogen explosions and/or

venting operations of units 1 and 3 (March 12 and 13/14) may have also resulted in significant releases. Because of the meteorological situation, these releases have been quickly blown towards the Pacific Ocean (especially the release of March 12) and may not have been significantly measured by the JPP38 station and the stations network located in the vicinity of the NPP. Total atmospheric releases of Cs-137 and I-131 aerosols estimated from long range simulation are found to be 1×10^{16} and 1×10^{17} Bq, respectively. By neglecting gas/particulate conversion phenomena, the total release of I-131 (gas + aerosol) could be 4×10^{17} Bq. Emissions estimated using JPP38 measurements are higher but uncertainties could be significant (total releases are ~ 5 – 7 larger regarding the long range results). The amounts of Cs-137 and I-131 emitted into the atmosphere during the Fukushima accident could represent 10 % of the Chernobyl accident releases (estimated to be 8.5×10^{16} Bq of Cs-137 and 1.8×10^{18} Bq of I-131).

Acknowledgments

The authors wish to thank the Comprehensive Nuclear-Test-Ban Treaty Organisation for fruitful discussions about the data collected by radionuclide stations of the International Monitoring Network during this event. A special thank you should be expressed to Harry Dupont of the Alten Company for his expertise and for the implementation of dispersion and mesoscale meteorological models.

Appendix

Figure 17 shows the IMS stations (International Monitoring System) closest to the Fukushima Dai-ichi NPP. These stations are JPP38 - Takasaki; Japan (~ 210 km) and RUP58 - Ussuriysk; Russia Fed. ($\sim 1,100$ km). The Fukushima Dai-ichi site and the city of Tokyo are also indicated on the map. Figures 18 and 19 show the IMS networks of radionuclide (aerosols) and noble gas stations in their September 2011 operational states.

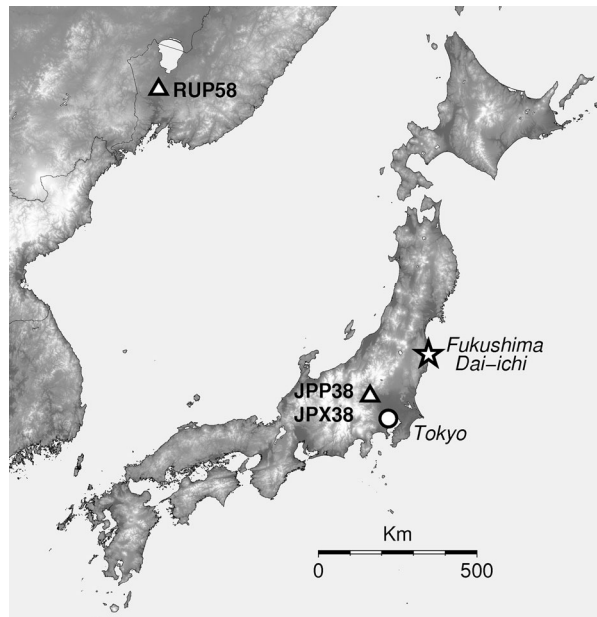


Figure 17
Location of IMS stations (triangles) situated close to the Fukushima Dai-ichi plant (star)



Figure 18
Particulate stations of the International Monitoring System (state of the network in March 2011). White circles operational stations. Dark squares non operational stations



Figure 19

Noble gas stations of the International Monitoring System (state of the network in March 2011). Circles SAUNA systems. Triangles SPALAX systems. Inverted triangles ARIX systems. Dark squares non operational stations

REFERENCES

- ACHIM, P., GROSS, P., LE PETIT, G., TAFFARY, T. and ARMAND, P. (2011), Contribution of Isotopes Production Facilities and Nuclear Power Plants to the Xe-133 Worldwide Atmospheric Background. CTBT Science and Technology, June 8 to 10, Vienna, Austria.
- BIOsphere Modelling and ASSESSment (BIOMASS) programme: Testing of environmental transfer models using data from the atmospheric release of Iodine-131 from the Hanford site, USA, in 1963. Report of the Dose Reconstruction Working Group of the Biomass Programme, Theme 2. International Atomic Energy Agency, Vienna, March 2003.
- CAPUT, C., CAMUS, H., GAUTHIER, D., and BELOT, Y. (1993), *Experimental study of washout of iodine vapour scavenged by rain* (in French). Radioprotection Volume 28, Number 1, January–March.
- CHINO, M., NAKAYAMA, H., NAGAI, H., TERADA, H., KATATA, G., and YAMAZAWA, H. (2011), *Preliminary estimation of release amounts of ^{131}I and ^{137}Cs accidentally discharged from the Fukushima Daiichi nuclear power plant into the atmosphere*. Journal of Nuclear Science and Technology, Vol. 48, No. 7, 1129–1134.
- DOE, US Department of Energy and National Nuclear Security Administration (NNSA), (2011) Radiological assessment of effects from Fukushima Daiichi power plant. Radiation monitoring data updated from March 22 to May 13.
- FAST, J. D., and EASTER, R. C. A. (2006), Lagrangian particle dispersion model compatible with WRF. 7th Annual WRF User's Workshop, 19–22 June, Boulder, CO.
- FLEXPART and FLEXTRA homepage at the Norwegian Institute for Air Research (NILU). <http://transport.nilu.no/flexpart>.
- KALINOWSKI, M.B., and TUMA, M.P. (2009), *Global radioxenon emission inventory based on nuclear power reactor reports*. Journal of Environmental Radioactivity 100, 58–70.
- KANEYASU, N., OHASHI, H., SUZUKI, F., OKUDA, T., and IKEMORI, F. (2012), *Sulfate Aerosol as a Potential Transport Medium of Radiocesium from the Fukushima Nuclear Accident*. Environmental Science & Technology, 46, 5720–5726.
- KATATA, G., OTA, M., TERADA, H., CHINO, M., and NAGAI, H. (2012), *Atmospheric discharge and dispersion of radionuclides during the Fukushima Dai-ichi Nuclear Power Plant accident. Part I: Source term estimation and local-scale atmospheric dispersion in early phase of the accident*. Journal of Environmental Radioactivity 109, 103–113.
- KATATA, G., TERADA, H., NAGAI, H., and CHINO, M. (2012), *Numerical reconstruction of high dose rate zones due to the Fukushima Dai-ichi Nuclear Power Plant*. Journal of Environmental Radioactivity 111, 2–12.
- LE PETIT, G., DOUYSSET, G., DUCROS, G., GROSS, P., ACHIM, P., MONFORT, M., RAYMOND, P., PONTILLON, Y., JUTIER, C., BLANCHARD, X., TAFFARY, T., and MOULIN, C. (2012), *Analysis of radionuclide releases from the Fukushima Dai-ichi Nuclear Power Plant*

- accident, Part I*, Pure Appl. Geophys. doi:10.1007/s00024-012-0581-6
- MEXT, Ministry of Education, Culture, Sports, Science and Technology—Japan: Reading of environmental radioactivity level by prefecture, Time series data.
- MM5, Modeling System Version 3. PSU/NCAR mesoscale modeling system. Tutorial Class Notes and User's Guide, January 2005.
- MASSON, O., *et al.* (2011), *Tracking of Airborne Radionuclides from the Damaged Fukushima Dai-ichi Nuclear Reactors by European Networks*. Environmental Science & Technology, Vol 45, 7670–7677.
- MATHIEU, A., KORSAKISSOK, I., QUÉLO, D., GROËLL, J., TOMBETTE, M., DIDIER, D., QUENTRIC, E., SAUNIER, O., BENOIT, J.P., and ISNARD, O. (2012), *Atmospheric Dispersion and Deposition of Radionuclides from the Fukushima Daiichi Nuclear Power Plant Accident*. Elements, Vol. 8, 195–200.
- MATTHEWS, M. (2010), Workshop on Signatures of Medical and Industrial Isotopes Production (WOSMIP)—A Review. US DOE Report PNNL-19294, February 2010.
- NCEP/GFS meteorological data at global scale. <http://weather.noaa.gov/pub/SL.us008001/ST.opnl>.
- NISA, Japanese Nuclear and Industrial Safety Agency: Bulletins on conditions of Fukushima Daiichi Nuclear Power Station. <http://www.nisa.meti.go.jp/english/press/index.html>.
- OKADA, S. (2011), Off-Site Activities regarding the Accident at the Fukushima Daiichi Nuclear Power Station and Lesson from Them. World Engineers' Convention, Geneva, 4–9 September.
- PITTAUEROVÁ, D., HETTWIG, B., and FISCHER, W. (2011), *Fukushima fallout in Northwest German environmental media*. Journal of Environmental Radioactivity, 102, 877–880.
- QIAO, F.L., WANG, G.S., ZHAO, W., ZHAO, J.C., DAI, D.J., SONG, Y.J., and SONG, Z.Y. (2011), *Predicting the spread of nuclear radiation from the damaged Fukushima Nuclear Power Plant*. Chinese Science Bulletin Vol. 56, No. 18, 1890–1896.
- QUÉLO, D., GROËLL, J., DIDIER, D., MATHIEU, A., KORSAKISSOK, I., TOMBETTE, M., QUENTRIC, E., BENOIT, J.P., and ISNARD, O. (2011), Atmospheric transport modeling and situation assessment of the Fukushima accident. 15th annual GMU conference on atmospheric transport & dispersion modeling, July 12–14, Fairfax, Virginia, U.S.A.
- SEHMEL, G.A. (1980), *Particle and gas dry deposition: a review*. Atmospheric Environment Vol. 14, pp. 983–1011.
- SLINN, W.G.N. (1982), *Predictions for particle deposition to vegetative canopies*. Atmos. Environ., 16, 1785–1794.
- STOHL, A., HITTENBERGER, M., and WOTAWA, G. (1998), *Validation of the Lagrangian particle dispersion model FLEXPART against large-scale tracer experiment data*. Atmos. Environ. 32, 4245–4264.
- STOHL, A., SEIBERT, P., WOTAWA, G., ARNOLD, D., BURKHART, J.F., ECKHARDT, S., TAPIA, C., VARGAS, A., and YASUNARI, T.J. (2012), *Xenon-133 and caesium-137 releases into the atmosphere from the Fukushima Dai-ichi nuclear power plant: determination of the source term, atmospheric dispersion, and deposition*. Atmospheric Chemistry and Physics, 12, 2313–2343.
- TAKEMURA, T., NAKAMURA, H., TAKIGAWA, M., KONDO, H., SATOMURA, T., MIYASAKA, T., and NAKAJIMA, T. (2011), *A Numerical Simulation of Global Transport of Atmospheric Particles Emitted from the Fukushima Daiichi Nuclear Power Plant*. SOLA, Vol. 7, 101–104.
- TEPCO Press releases. <http://www.tepco.co.jp/en/nu/press/f1-np/index-e.html>.
- TERADA, H., KATATA, G., CHINO, M., and NAGAI, H. (2012), *Atmospheric discharge and dispersion of radionuclides during the Fukushima Dai-ichi Nuclear Power Plant accident. Part II: verification of the source term and analysis of regional-scale atmospheric dispersion*. Journal of Environmental Radioactivity 112, 141–154.
- UNSCEAR: *Exposures and effects of the Chernobyl accident*. Annex J. Report Vol 2, 456–457, (2000).
- UEMATSU, M., MERRILL J.T., PATTERSON T.L., DUCE, R.A., and PROSPERO J.M. (1988), *Aerosol residence time and iodine gas/particle conversion over the North Pacific as determined from Chernobyl radioactivity*. Geochemical Journal, Vol. 22, 157–163.
- WESELY, M.L. and HICKS, B.B. (1977), *Some factors that affect the deposition rates of sulfur dioxide and similar gases on vegetation*. J. Air Poll. Contr. Assoc., 27, 1110–1116.
- WINIAREK, V., BOCQUET, M., SAUNIER, O., and MATHIEU A. (2012), *Estimation of Errors in the Inverse Modeling of Accidental Release of Atmospheric Pollutant: Application to the Reconstruction of the Cesium-137 and Iodine-131 Source Terms from the Fukushima Daiichi Power Plant*. Journal of Geophysical Research, doi:10.1029/2011JD016932.
- WRF, Weather Research and Forecasting Model. <http://www.wrf-model.org/index.php> and <http://www.mmm.ucar.edu/wrf/users>.